Journal of Alloys and Compounds 601 (2014) 63–66

Contents lists available at ScienceDirect

Journal of Alloys and Compounds

journal homepage: www.elsevier.com/locate/jalcom

# Effects of Ti interlayers on microstructures and hydrogen storage capacity in Mg/Pd multilayer thin films

Hwaebong Jung [a], Junhan Yuh [b], Sungmee Cho [a,*], Wooyoung Lee [a,*]

[a] Department of Materials Science and Engineering, Yonsei University, 262 Seongsanno Seodaemun-gu, Seoul 129-749, Republic of Korea
[b] New Growth Technology Strategy Department, Corporate Technology Division, POSCO, POSCO Center, 892 Daechi 4 dong, Gangnam-gu, Seoul 135-777, Republic of Korea

ARTICLE INFO

*Article history:*
Received 27 January 2014
Received in revised form 17 February 2014
Accepted 18 February 2014
Available online 26 February 2014

*Keywords:*
Hydrogen storage materials
Ti interlayer
Mg–Pd multilayer thin film

ABSTRACT

In this work, we examine the microstructural and hydrogen storage properties of 60 multilayer Mg/Pd and Ti/Mg/Ti/Pd films using an ultra-high-vacuum (UHV) DC magnetron sputtering system. The hydrogen absorption capacity of the Ti/Mg/Ti/Pd film was found to be 1.7, 3.5, and 4.7 wt% at 50, 100, and 150 °C, respectively, while that of the Mg/Pd film was measured at significantly lower values, 0.18, 0.65, and 1.35 wt%. The hydrogen absorption capacity for the Mg/Pd and Ti/Mg/Ti/Pd films is greatly dependent upon the formation of Mg–Pd intermetallic phases, formed during the hydrogenation process. Our results demonstrate that Ti interlayers in the Ti/Mg/Ti/Pd film play a crucial role in preventing the formation of Mg–Pd intermetallic phases, which originate from the inter-diffusion of Mg and Pd atoms during hydrogenation, and thus result in an improved hydrogen storage capacity.



## 1. Introduction

Magnesium (Mg) has recently drawn significant attention as a promising candidate material for future hydrogen storage applications, due to its low cost and relatively high reversible hydrogen storage capacity (7.6 wt%, $MgH_2$). However, bulk $MgH_2$ is limited in its ability to release hydrogen due to its high hydrogen-desorption temperature (>350 °C), high thermodynamic stability ($\Delta H = -75$ kJ/mol), and slow hydrogenation/dehydrogenation kinetics [1]. Thus, alternative approaches have been studied to improve the reaction kinetics of Mg and Pd, and decrease hydrogen desorption temperatures. These include Mg-based, bulk powder-ball milling [2,3], additives [4,5], catalysts [6–9], and Mg-based thin films [10–26]. Among these techniques, the Mg-based thin films with 3d-transition metals are reported to reduce absorption/desorption hydrogen temperatures and enhance hydrogenation/dehydrogenation properties.

Mg/Pd bilayer films [10–16] were studied, as Pd is known to not only protect Mg from oxidation in the Mg/Pd films, but also to function as a catalyst, facilitating hydrogenation kinetics by improving the hydrogen storage performance of Mg. Poor hydrogenation kinetics were observed, however, due to the formation of binary intermetallic Mg–Pd alloys at the interface between the Mg and Pd layers [12,15]. Recently, Mg-based trilayer films such as MgAl [21], MgNi [22], and Mg-based multilayer films such as MgTi [24,25,27] and MgFeTi [20] have also been reported to improve the hydrogenation of Mg at lower temperatures. These films have also been utilized to explain the role of hydrogen solution enthalpy in the transition metal layer as it relates to hydrogen absorption/desorption kinetics.

In this paper, we have investigated the effects of Ti interlayers on the microstructures and hydrogen storage capacity of Mg/Pd multilayer thin films. We intend to utilize a Ti interlayer between the Mg and Pd to enhance the hydrogen storage capacity, as well as to prevent interdiffusion at the Mg/Pd interface during the hydrogenation process at elevated temperatures. We found that the overall hydrogen absorption capacity of a Ti/Mg/Ti/Pd multilayer film obtained at 50, 100, and 150 °C was significantly larger than that of a Mg/Pd multilayer film without Ti interlayers. We discuss how to enhance the hydrogen storage capacity in the Mg/Pd multilayer films by inserting a Ti interlayer between the Mg and Pd layers, preventing the formation of Mg–Pd intermetallic phases originating from the inter-diffusion of Mg and Pd.

## 2. Experiment

The depositions of 60 multilayers composed of Mg(360)/Pd(40) and Ti(10)/Mg(360)/Ti(10)/Pd(40) thin films (in nm) were conducted via ultra-high-vacuum (UHV) DC magnetron sputtering, on a glass substrate (25 × 75 mm) in Ar atmosphere. The base pressure was $4 \times 10^{-8}$ Torr, and the deposition process was carried out below $2.3 \times 10^{-3}$ Torr with a 34 sccm Ar flow. The details of the deposition process were explained by Lee et al. [28]. Typical deposition rates of multilayer films at room temperature (RT) were ~12.9 Å/s for Mg at 50 W, ~1.7 Å/s for Ti at

* Corresponding authors. Tel.: +82 0221232834; fax: +82 023125375 (W. Lee).
*E-mail addresses:* csmise@yonsei.ac.kr (S. Cho), wooyoung@yonsei.ac.kr (W. Lee).

http://dx.doi.org/10.1016/j.jallcom.2014.02.105
0925-8388/

50 W and ~4 Å/s for Pd at 20 W. The purity of the Mg, Ti, and Pd targets was 4 N. All samples were easily peeled from the glass substrates following deposition, as the glass with the Pd film had weak adhesion. Multilayer samples were heated from ambient temperature to 200 °C for 2 h in $H_2$ at a rate of 3 °C/min.

X-ray diffraction (XRD) was performed using an Ultima IV/ ME 200DX (Rigaku), and Transmission Electron Microscopy (TEM) was carried out using a JEM-2100F (JEOL). Prior to cross-sectional TEM observation, the samples were sliced in a direction perpendicular to the surface using a focused ion beam system (FIB, Quanta 3D FEG-FED). Hydrogen uptake measurements were carried out using a magnetic suspension microbalance (Rubotherm, Isosorp) via a gravimetric method performed under a vacuum pressure range up to 40 bar and temperature range of 50–150 °C. The amount of sample used for the measurements was 0.1–0.3 g. All sorption isotherms were obtained using ultrahigh purity gases ($H_2$: 99.999%; He: 99.99%).

## 3. Results and discussion

Fig. 1 presents the XRD patterns of a Mg/Pd multilayer thin film and a Ti/Mg/Ti/Pd multilayer thin film before and after hydrogenation at 200 °C for 2 h. Fig. 1(a) indicates the formation of both the Mg hexagonal phase (JCPDS: #35-0821) and Pd cubic phase (JCPDS: #46-1043). Following exposure to $H_2$ at 200 °C for 2 h, this Mg/Pd film shows significant changes in the phases present, with the appearance of $MgH_2$, $Mg_5Pd_2$, and $Mg_6Pd$ intermetallic compounds, as shown in Fig. 1(b). These secondary phases are presumably a result of the reaction between a Pd surface layer and the underlying Mg film, and are caused by the interdiffusion of Mg and Pd atoms. Given the lightness of Mg, it is assumed that the Mg atoms can diffuse significantly faster than the Pd atoms. In Fig. 1(c), the dominant XRD peaks of the as-deposited Mg/Pd film with the Ti interlayer are from Mg, Pd, and the hexagonal Ti (JCPDS: #44-1294) crystal structures, with an overlap of strong peaks corresponding to the Pd (111) and Ti (101) planes. After exposure of the Ti/Mg/Ti/Pd film to $H_2$ under the above conditions, no intermetallic Mg–Pd peaks were observed (with the exception of $MgH_2$ as a hydrogen storing phase in the film), as shown in Fig. 1(d). Our results indicate that the Ti interlayers effectively protect against the interdiffusion of Mg–Pd alloys; however, some intermixing of layers occurred forming a negligible intermetallic $TiPd_3$ phase.

Fig. 2 shows cross-sectional TEM images of the multilayered Mg/Pd and Ti/Mg/Ti/Pd films. The average layer thicknesses of the Mg and Pd films in the TEM image are ~40 nm and ~16 nm, respectively. As shown in Fig. 2(a), the films show dense, clear, and smooth layers with no intermixing observed during deposition. Interestingly, the Mg/Pd sample annealed in hydrogen for 2 h at 200 °C can be distinguished via two distinct regimes (see Fig. 2(b)), which are clearly-observed intermetallic compounds such as $Mg_xPd_y$ phase (marked arrows) in the film. We infer that regime 1 drives the interdiffusion of Mg and Pd through the diluted alloy at regime 2 during annealing, with the subsequent formation of $Mg_5Pd_2$ (regime 1) and $Mg_6Pd$ (regime 2) resulting from a temperature gradient under $H_2$ flow, as shown in Fig. 2(c). This is in good agreement with the XRD results shown above. Both Fig. 2(c and d) shows cross-sectional TEM images of a Ti/Mg/Ti/Pd film after exposure to $H_2$ at 200 °C for 2 h. Fig. 2(c) displays well-layered films with slightly wavy lines. The EDS line scan profiles (inset in Fig. 2(c)) also indicate that the Ti interlayers can play a role as an effective barrier layer due to the immiscibility of the Mg–Pd alloys. The high-resolution TEM image demonstrates obvious Ti/Mg/Ti/Pd layers with no interdiffusion, as seen in Fig. 2(d).

Fig. 3 illustrates the schematics of (a) the Mg/Pd and (b) Ti/Mg/Ti/Pd thin films before and after hydrogenation at 200 °C, based on TEM observations. The as-deposited Mg/Pd film on the substrate shows multiple Mg and Pd layers, whereas new phases appear in the film during annealing in $H_2$ at 200 °C, such as the formation of the $Mg_xPd_y$ phases, $Mg_6Pd$ and $Mg_5Pd_2$, as sketched in Fig. 3(a). The addition of the Ti interlayers is believed to effectively prevent intermixing between the Mg and Pd layers (see Fig. 3(b)). Both the Ti and Pd layers can also function as effective catalysts for hydrogen dissociation and recombination.

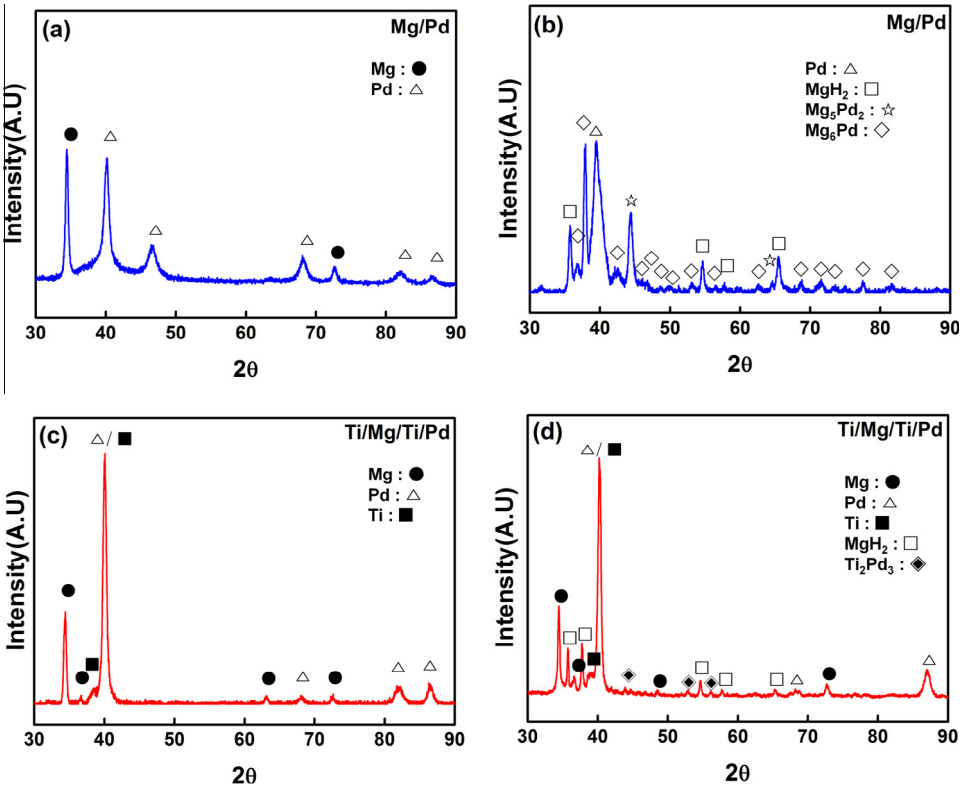


**Fig. 1.** XRD patterns of Mg/Pd and Ti/Mg/Ti/Pd multilayer films before and after hydrogenation at 200 °C for 2 h.

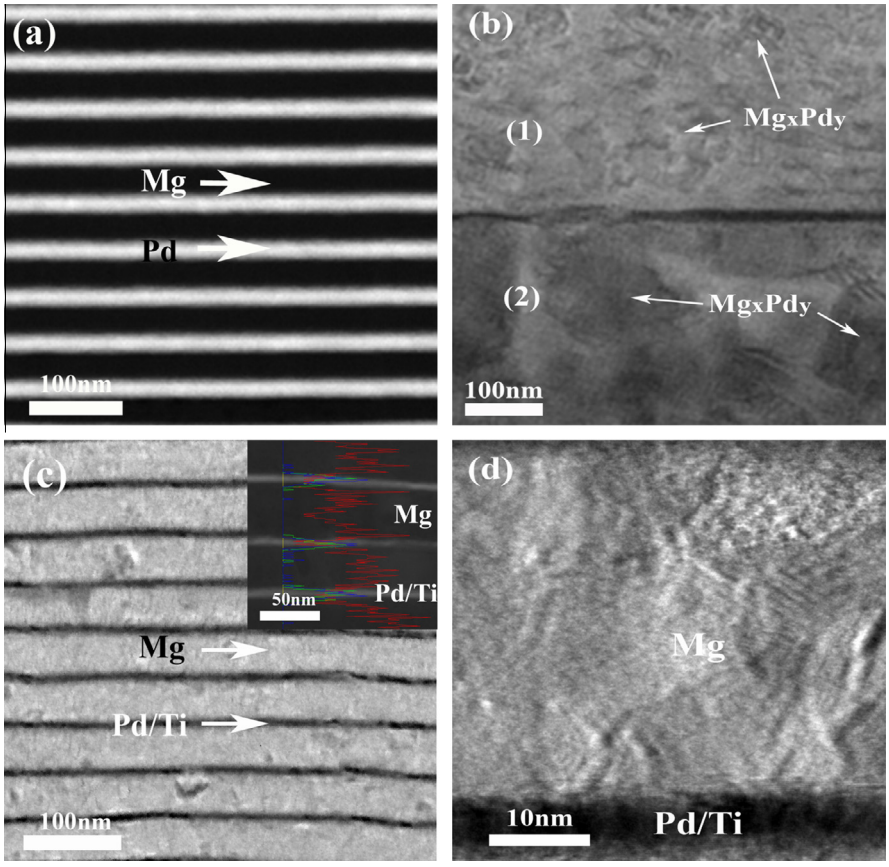


**Fig. 2.** Cross-sectional TEM images of (a) an as-deposited Mg/Pd multilayer film, (b) the Mg/ Pd multilayer film after hydrogenation, (c) low-resolution (inset: EDS line scan profiles) and (d) high-resolution images of a Ti/Mg/Ti/Pd multilayer film after hydrogenation at 200 °C.

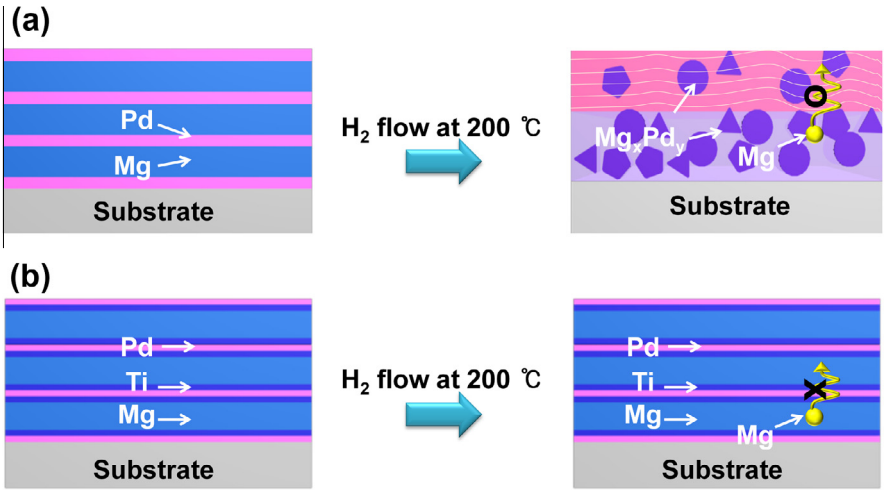


**Fig. 3.** Schematic diagrams of (a) a Mg/Pd multilayered film and (b) a Ti/Mg/Ti/Pd multilayer film on a substrate, before and after hydrogenation at 200 °C.

For the hydrogen storage capacity measurements, 60 multilayer Mg(360)/Pd(40) and Ti(10)/Mg(360)/Ti(10)/Pd(40) thin films (in nm) were delaminated from substrates, and then tested under a vacuum below 40 bar at 150, 100, and 50 °C, in serial order. Fig. 4 illustrates the hydrogen absorption properties of (a) the Mg/Pd and (b) Ti/Mg/Ti/Pd films as a function of pressure. Fig. 4(a) shows a plot of the hydrogen gas pressure isotherm versus hydrogen absorption capacity for the Mg/Pd film, indicating hydrogen absorption capacities of 0.18, 0.65, and 1.35 wt% at 50, 100, and 150 °C, respectively. Lower values for the hydrogen absorption capacity were found at each temperature when compared to the theoretical capacity of $MgH_2$ which indicates a decrease in hydrogen storage. This is fundamentally due to the formation of $Mg_6Pd$ and $Mg_5Pd_2$ phases. Such Mg–Pd alloy phases are likely to contribute to a decrease in the interfacial free energy between the Mg and Pd layers, leading to structural instability in the multilayered film [24].

As compared to the Mg/Pd film without the Ti interlayers, the absorption capacities in a Ti/Mg/Ti/Pd film are found to be 1.7, 3.5, and 4.7 wt% at 50, 100, and 150 °C, respectively, as shown in

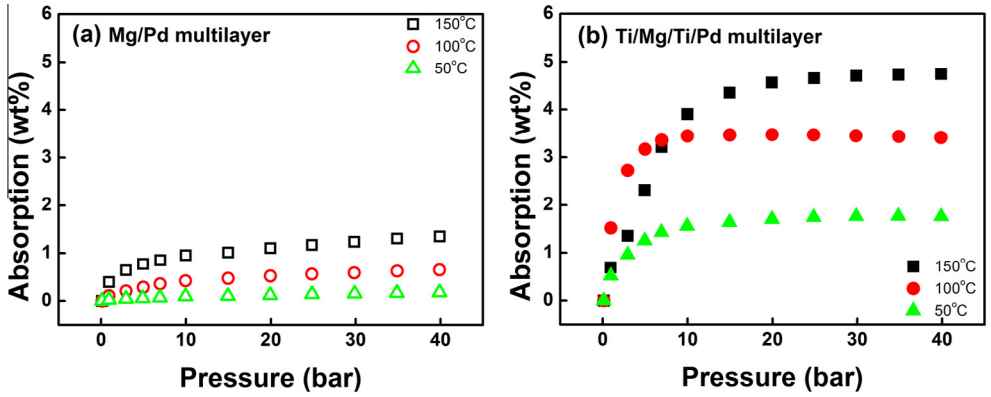


**Fig. 4.** Hydrogen absorption capacity of (a) a Mg/Pd multilayered film and (b) a Ti/Mg/Ti/Pd multilayered film as a function of pressure at 50, 100, and 150 °C.

Fig. 4(b). Accordingly, the overall hydrogen absorption capacities of the Ti/Mg/Ti/Pd films obtained at 50, 100, and 150 °C were significantly larger than those of the Mg/Pd films without the Ti interlayers. We found that the hydrogen absorption capacity (3.5 wt%) of the Ti/Mg/Ti/Pd film in this study is higher than that of a Mg/Pd film (2.6 wt%) reported in a previous study [15] at the same temperature, 100 °C. The formation of Mg/Pd alloys during the hydrogenation process at elevated temperatures prevents the formation of $MgH_2$, resulting in a lower Mg/Pd film hydrogen storage capability. On the other hand, the higher hydrogen storage capacity of the Ti/Mg/Ti/Pd film is attributed to the Ti interlayers playing the role of an effective blocking layer between the Mg and Pd layers. The extra interfacial energy in the Ti interlayers is likely to decrease the energy barrier required for the formation of $MgH_2$ at the interface [24], providing microstructural stability during hydrogen absorption-desorption.

## 4. Conclusions

We have fabricated 60 multilayers composed of Mg/Pd and Ti/Mg/Ti/Pd films using an ultra-high-vacuum (UHV) DC magnetron sputtering system in order to measure the hydrogen storage capacity. The hydrogen absorption capacities of the Ti/Mg/Ti/Pd film are 1.7, 3.5, and 4.7 wt% at 50, 100, and 150 °C, respectively, while those of the Mg/Pd film are significantly lower, 0.18, 0.65, and 1.35 wt%, respectively, due to the formation of Mg–Pd intermetallic phases during the hydrogenation process. XRD and TEM confirmed the existence of these Mg–Pd intermetallic phases, which are detrimental to hydrogen storage, in the Mg/Pd film without Ti interlayers after exposure to $H_2$ at 200 °C. No Mg–Pd intermetallic phases were observed in the Ti/Mg/Ti/Pd film after hydrogenation, indicating that a Ti interlayer between the Mg and Pd layers can prevent the formation of Mg–Pd intermetallic phases originating from the inter-diffusion of Mg and Pd during hydrogenation. We conclude that the hydrogen storage capacity in the Mg/Pd multilayer films can be significantly enhanced by inserting a Ti interlayer between the Mg and Pd. The Ti interlayer plays the important role of blocking the inter-diffusion of Mg and Pd atoms during hydrogenation at elevated temperatures.

## Acknowledgements

This work was supported by the POSCO Research Project (2013Z048,), Priority Research Centers Program (2009-0093823), and the Pioneer Research Center Program (2013008070) through the National Research Foundation of Korea (NRF).

## References

[1] A.M. Seayad, D.M. Antonelli, Adv. Mater. 16 (2004) 765.
[2] L. Zaluski, A. Zaluska, J.O. Strom-Olsen, J. Alloys Comp. 217 (1995) 245–249.
[3] A. Zaluska, L. Zaluski, J.O. Ström-Olsen, J. Alloys Comp. 289 (1999) 197.
[4] N. Bazzanella, R. Checchetto, A. Miotello, Appl. Phys. Lett. 92 (2008) 051910.
[5] S. Orimo, K. Ikeda, H. Fujii, Y. Fujikawa, Y. Kitano, K. Yamamoto, Acta Mater. 45 (1997) 2271.
[6] N. Hanada, T. Ichikawa, H. Fujii, J. Phys. Chem. B 109 (2005) 7188.
[7] M. Dornheim, S. Doppiu, G. Barkhordarian, U. Boesenberg, T. Klassen, O. Gutfleisch, R. Bormann, Scripta Mater. 56 (2007) 841–846.
[8] L. Xie, Y. Liu, Y.T. Wang, J. Zheng, X.G. Li, Acta Mater. 55 (2007) 4585.
[9] M. Polanski, J. Bystrzycki, J. Alloys Comp. 486 (2009) 697–701.
[10] G.L.N. Reddy, S. Kumar, Y. Sunitha, S. Kalavathi, V.S. Raju, J. Alloys Comp. 481 (2009) 714–718.
[11] S. Barcelo, M. Rogers, C.P. Grigoropoulos, S.S. Mao, J. Hydrogen Energy 35 (2010) 7232–7235.
[12] S. Singh, S.W.H. Eijt, M.W. Zandbergen, W.J. Legerstee, V.L. Svetchnikov, J. Alloys Comp. 441 (2007) 344–351.
[13] K. Higuchi, H. Kajioka, K. Toiyama, H. Fujii, S. Orimo, J. Alloys Comp. 293–295 (1999) 484–489.
[14] K. Higuchi, K. Yamamoto, H. Kajioka, K. Toiyama, M. Honda, S. Orimo, H. Fujii, J. Alloys Comp. 330–332 (2002) 526–530.
[15] S.Y. Yea, S.L.I. Chan, L.Z. Ouyang, M. Zhu, J. Alloys Comp. 504 (2010) 493–497.
[16] S. Bouhtiyya, L. Roue, Int. J. Hydrogen Energy 34 (2009) 5778–5784.
[17] T.J. Richardson, J.L. Slack, R.D. Armitage, R. Kostecki, B. Farangis, M.D. Rubin, Appl. Phys. Lett. 78 (2001) 3047.
[18] A. Borgschulte, R.J. Westerwaal, J.H. Rector, B. Dam, R. Griessen, Schoenes, Phys. Rev. B 70 (2004) 155414.
[19] A. Borgschulte, R. Gremaud, S. Man, R.J. Westerwaal, J.H. Rector, B. Dam, R. Griessen, Appl. Surf. Sci. 253 (2006) 1417.
[20] D.M. Borsa, A. Baldi, M. Pasturel, H. Schreuders, B. Dam, R. Griessen, Appl. Phys. Lett. 88 (2006) 241910.
[21] G. Garcia, R. Domenech-Ferrer, F. Pi, J. Santiso, Rodriguez-Viejo, J. Comb. Chem. 9 (2007) 230–236.
[22] M. Pasturel, R.J. Wijngaarden, W. Lohstroh, H. Schreuders, M. Slaman, B. Dam, Chem. Mater. 19 (2007) 624–633.
[23] X. Tan, C.T. Harrower, B.S. Amirhiz, D. Mitlin, Int. J. Hydrogen Energy 34 (2009) 7741–7748.
[24] G. Xin, J. Yang, H. Fu, W. Li, J. Zheng, X. Li, RSC Adv. 3 (2013) 4167–4170.
[25] A. Baldi, G.K. Pálsson, Gonzalez-Silveira, Schreuders, Slaman, J.H. Rector, G. Krishnan, B.J. Kooi, G.S. Walker, M.W. Fay, B. Hjörvarsson, R.J. Wijngaarden, B. Dam, R. Griessen, Phys. Rev. B 81 (2010) 224203.
[26] P. Mengucci, G. Barucca, G. Majni, N. Bazzanella, R. Checchetto, A. Miotello, J. Alloys Comp. 509S (2011) S572–S575.
[27] G. Xin, J. Yang, C. Wang, J. Zheng, X. Li, Dalton Trans. 41 (2012) 6783–6790.
[28] J. Lee, W. Shim, E. Lee, J.S. Noh, W. Lee, Angew. Chem. 123 (2011) 5413–5417.